Pergamon

Int. J. Heat Mass Transfer. Vol. 39, No. 9, pp. 1911–1923, 1996

0017-9310/96 $15.00+0.00

0017–9310(95)00269–3

Jet impingement drying of a moist porous solid

NICHOLAS D. FRANCIS
Sandia National Laboratories, P.O. Box 5800, MS-1326, Albuquerque, NM 87185-1326, U.S.A.

and

WILLIAM J. WEPFER
The George W. Woodruff School of Mechanical Engineering, Georgia Institute of Technology, Atlanta, GA 30332, U.S.A.

(*Received* 23 *September* 1994 *and in final form* 10 *July* 1995)

Abstract—This paper investigates the thermal characteristics of a continuous industrial drying process for semi-porous textile composites. The conservation of mass, momentum and energy are written for a partially saturate porous fiber layer attached to a solid-backing layer. The numerical solution of the one-dimensional and transient conservation equations provides the temperature, volumetric saturation and gas phase pressure distributions in the moist porous solid and the temperature distribution in the solid-backing layer. During the wet region drying period, continuous liquid exists in the pore space, the moisture transport within the solid is described by the Darcy form of the momentum equation. The moisture transport in the sorption region is described by a bound liquid diffusion and gas phase transport. For the jet impingement type dryer, it is assumed that the penetration of the flow field into the porous solid is small (assumed valid due to the presence of the solid backing). The enhanced transport coefficients at the drying surface are estimated with the use of the Kolmogoroff theory of isotropic turbulence. This theory provides correlations for the heat and mass transfer coefficients from the fluid properties and the turbulent energy dissipation rate in the fluid. The model results of the continuous industrial drying process are compared to independent experimental temperature and global moisture content measurements taken in an operational industrial dryer. From the model analysis and experimental data, the heat flux conditions at the drying surface dictate the manner in which the solid is dried. The heat transfer coefficients considered are in the range of 20–130 $W\ m^{-2}\ K^{-1}$ and necessarily affect the manner in which moisture transport occurs within the solid. It is seen that the lower heat transfer coefficients more accurately represent the internal transport phenomena occurring during the drying process and the heating of the solid. The transport coefficients are compared to previously obtained empirical results.

INTRODUCTION

Industrial drying processes are energy intensive and represent a major factor in the cost of producing many consumer goods. Industrial drying applications include the production of textiles, paper and pulp, food industries and agricultural products, chemical products, building and construction materials, and many others.

This paper focuses on the drying needs and methods of the textile industry as they pertain to the production of modular carpet tiles. The solid-backed carpet tile is a moist porous composite subjected to a convection drying process. Determination of the drying characteristics of the material are necessary for dryer design and/or process control.

Hygroscopic capillary-porous media classify many textile products [1–6]. This solid group is characterized by moisture trapped in small and dead end pores. Solid classification is important particularly in the latter stages of drying; as it determines moisture and energy transport mechanisms. The physical quantification of a drying process, as indicated by authors [7–13], is obtained by performing mass, momentum, and energy balances on a differential control volume. Conservation of mass is written for the liquid phase as well as the gas phase. Also, mass continuity is written for each species present in the control volume: water vapor and air (binary mixture of ideal gases). The Darcy form of the momentum equation is applied for low velocity flows in porous solids. Species velocities are written with respect to the mass average velocity of the gas phase [14–16]. Finally, the conservation of energy equation is written for a multi-component, multi-phase porous medium. The conservation equations written for the partially saturated porous material (i.e. carpet fiber) establish the moisture concentration, temperature, and gas phase pressure, as a function of space and time.

The development of an evaporation front will occur when the moisture content approaches the maximum sorption or critical moisture content. While the evaporation front is maintained at the drying surface, liquid mass transfer occurs according to Darcy's law. This process is called wet region drying. During the wet region drying regime the liquid phase and the flow

NOMENCLATURE

c_p	constant pressure specific heat [J kg^{-1} K^{-1}]
C_l	surrounding fluid turbulence dissipation coefficient
D	molecular diffusion of water vapor in air [m^2 s^{-1}]
D_b	bound liquid water conductivity [m^2 s^{-1}]
E_d	activation energy [J kmol^{-1}]
g	gravitational constant [m s^{-2}]
h	enthalpy [J kg^{-1}]
Δh_w	differential heat of sorption [J kg^{-1}]
$\bar{h}_m$	mass transfer coefficient at the drying surface [m s^{-1}]
$\bar{h}_T$	heat transfer coefficient at the drying surface [W m^{-2} K^{-1}]
$\bar{h}_l$	heat transfer coefficient at the solid-backing surface [W m^{-2} K^{-1}]
h_{vap}	latent heat of vaporization [J kg^{-1}]
H	nozzle array-to-porous solid product spacing [m]
K_{sat}	intrinsic permeability [m^2]
k	thermal conductivity [W m^{-1} K^{-1}]
k_{rg}	relative permeability of the gas phase
k_{rl}	relative permeability of the liquid phase
L	composite layer thickness [m]
$\dot{m}$	mass source term [kg m^{-3} s^{-1}]
M	molecular mass [kg kmol^{-1}]
N	total number of nozzles (holes) in the array
P	pressure [N m^{-2}]
Pr	Prandtl number
$\bar{R}$	universal gas constant [Nm kmol^{-1} K^{-1}]
Re	Reynolds number
S	volumetric saturation
Sc	Schmidt number
T	temperature [K]
t	time [s]
t_K	Kolmogoroff time scale [s]
v	internal fluid velocity [m s^{-1}]
V	velocity [m s^{-1}]
$\dot{W}_b$	blower power [W]
w	relative humidity
x	distance [m]
X	moisture content [kg moisture kg dry solid^{-1}].

Greek symbols

ε_t	rate of turbulent energy dissipation per unit mass of fluid [m^2 s^{-3}]
θ	dimensionless temperature
λ	pore size distribution index
μ	dynamic viscosity [Ns m^{-2}]
ν	kinematic viscosity [m^2 s^{-1}]
ρ	density [kg m^{-3}]
ϕ	porosity.

Subscripts

a	air
b	bound, backing-solid
belt	belt velocity
c	capillary, characteristic
d	dry solid
eff	effective
eq	equilibrium
g	gas phase
i	initial
j	jet velocity
l	liquid phase
n	zone number
s	solid
sr	sorption region
v	vapor phase
vs	vapor phase saturated
wr	wet region
1	attachment point, initial, solid-backing heat transfer surface
2	drying surface
∞	ambient medium.

Superscripts

*	maximum sorption volumetric saturation.

of liquid is continuous. As the front begins to recede from the drying surface, the moisture in the region behind the moving interface is no longer described by Darcy's law. This process is called sorption region drying. The sorption regime is characterized by a discontinuous liquid phase. Bound liquid transport occurs by a liquid diffusion mechanism with the gradient of the moisture content as the recommended driving force [1, 17]. Additionally, the enthalpy of the bound liquid in this 'dryout' region must reflect the differential heat of sorption [4, 10, 17–20]. The motion of the evaporation front that divides the porous material is a function of the thermodynamic and transport properties used to describe the independent drying regimes. These properties inherently describe the transport of mass and energy during the two-regime (wet and sorption) drying model. The internal flow of mass and heat are directly influenced by the drying conditions at the boundaries.

The continuous industrial drying process is speci-

fied by a multiple jet impingement flow boundary condition as indicated by Martin [21]. This flow field is commonly employed in industrial drying processes for enhanced drying rates. Flow field geometry and fluid properties establish the heat and mass transfer coefficients at the drying surface [22–29].

Experimental data have been obtained from a continuous industrial drying process. The drying experiments provided temperature data obtained at specific locations in the material for multiple oven temperatures, belt speeds, and initial moisture contents. The experimental moisture concentration data taken from the continuous dryer were obtained by removing the sample and weighing at different positions along the dryer length.

Many authors [12, 30–45] provide drying models for different porous solids that include: textiles, concrete slabs, burial of high level nuclear waste products, and flow through porous beds. In each case, the governing conservation equations were obtained and supplemented with the necessary thermodynamic and transport properties. In some cases, volumetric energy generation create massive internal temperature and pressure gradients that increase mass transfer by providing for very large bulk moisture transfer. In most of the cases reported, however, the boundary conditions for the drying processes are characterized by parallel flow type such that the drying medium flows parallel to the product being dried. Additionally, only limited experimental results are available for model calibration. In order to provide a baseline or calibration analysis for the jet impingement drying theory, experimental results of a batch drying process are compared to the drying theory developed by Francis [19]. The two-region conservation equations and transport and thermodynamic properties developed for the jet impingement analysis are applied to a simple batch drying (performed in a controlled laboratory dryer) analysis. The results of these analyses for the parallel air flow boundary conditions provide a bridge for building the numerical analysis of an operational industrial dryer.

Turbulent jet impingement flow field

The continuous feed industrial drying process is characterized by multiple turbulent jets impinging on the partially saturated porous solid. The physical characteristics of the turbulent flow field are obtained from the continuity equation, Navier–Stokes equations, and the energy equation, Polat *et al.* [46–48]. These fundamental equations are generally supplemented by the turbulence models. The one-equation model for high Reynolds numbers provides an additional equation for the turbulent kinetic energy of the flow field in terms of the turbulent length scales, viscosity, and dissipation rate, Polat *et al.* [46]. The two-equation model for high Reynolds numbers utilizes the equation established for the turbulent kinetic energy (the one-equation model) and provides for an additional governing equation for the turbulent energy dissipation rate. The subsequent two-dimensional governing conservation equations are coupled in the velocities, and the turbulent flow field properties such as the turbulence viscosity, length scale of turbulence dissipation, length scale of turbulence and other empirical constants.

It is possible to provide for correlation methods to obtain heat and mass transfer coefficients under extremely turbulent conditions [22–29, 49]. These methods have been previously applied to mixing vessels and agitated tanks, packed beds, pipe flow, open channel flow and many others. The heat and mass transfer coefficient expressions are obtained by introducing the concept of the rate of turbulent energy dissipation by the flow field. The Kolmogoroff theory of isotropic turbulence describes the viscous energy dissipation rate. The dissipation rate is then used to obtain the mass transfer coefficient for a given flow field. If a predetermined amount of mechanical energy is supplied to a turbulent flow field, the transition of this quantity is initially to kinetic energy of the integral or large scale eddies. The kinetic energy is then transferred to the smaller scale eddies where nearly all of the turbulence dissipation occurs. The geometrical nature of the equipment used to produce the turbulent flow field provides only a minor effect on the energy dissipation in the small scale eddies. The decay of the dissipation rate from the source (i.e. jets) is estimated with the use of a grid-generated turbulence model.

Grid-generated turbulence models are considered as a basis for the decay of the turbulent energy dissipation rate as generated from the flow source (i.e. the impinging jets). The Kistler *et al.* [50] model for grid-generated turbulence is written for very large mean free stream velocities similar to those found in the case of multiple impinging jets in an industrial drying process.

GOVERNING EQUATIONS FOR MASS, MOMENTUM AND ENERGY TRANSFER IN A POROUS MEDIUM

The governing equations of mass and energy transfer are written for the wet region and sorption region drying periods. During the initial stages of drying, the textile product is uniformly, partially saturated with moisture and the wet region conditions exist. The internal transport of liquid moisture is mainly by capillary flow and the liquid phase is essentially continuous. This presumes that evaporation occurs primarily at the drying surface ($x = L_2$ in Fig. 1). With continued drying, the moisture concentration at the drying surface is reduced to the maximum sorption moisture content and the evaporation front begins to recede from this surface into the porous solid. During the sorption region drying period, the bound moisture transport is governed by the gradient of the bound moisture content. The schematic of the two-region drying model is shown in Fig. 1. The drying regimes are shown separated by the moving evaporation front.

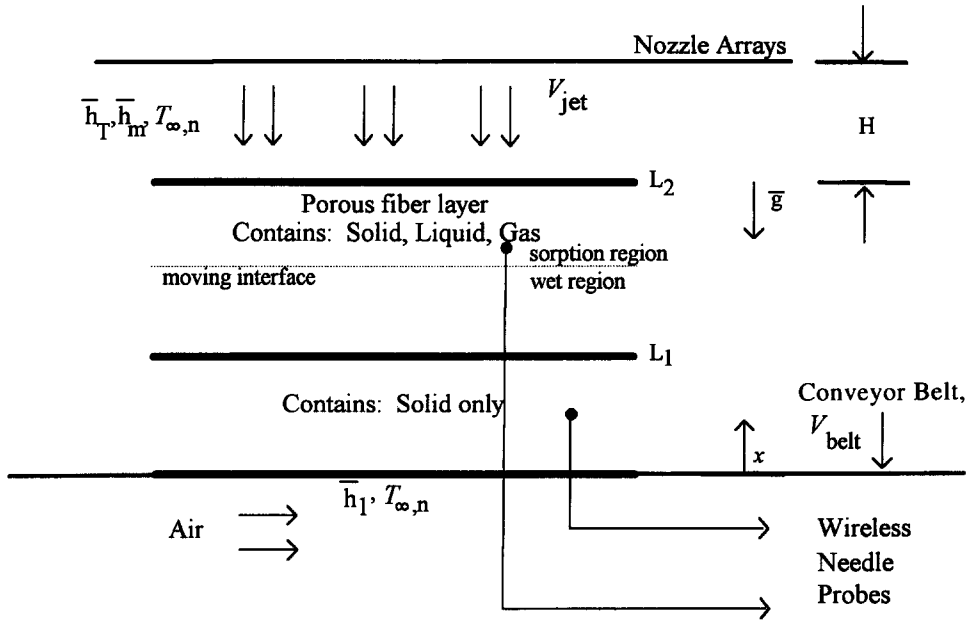

Fig. 1. The instrumented modular carpet tile, industrial dryer (not to scale).

Assumptions

(1) The material and its properties are macroscopically homogeneous.
(2) The solid phase is a rigid matrix, thermophysical properties are constants.
(3) Compressional work and viscous dissipation are negligible for each phase.
(4) Diffusional body force work and kinetic energy are small.
(5) The gas phase is a binary mixture of ideal gases.
(6) The three phase system is in local thermodynamic equilibrium.
(7) Gravity terms are important for liquid phase but not the gas phase.
(8) Fluids are Newtonian and the inertial effects are small.
(9) Drying medium (impingement air) does not penetrate the porous solid.

Conservation of mass, wet region

The conservation of liquid mass in terms of the volumetric saturation and the mass source term is obtained from a differential control volume in the moist porous solid as the following

$$\frac{\partial}{\partial t}(\phi S_l \rho_l) = -\frac{\partial}{\partial x}(\rho_l v_l) - \dot{m}. \tag{1}$$

The governing mass conservation equations for the porous solid during the wet region drying period are derived in detail [19]. Conservation of total water mass (liquid plus water vapor) is written in terms of the liquid and gas phase volumetric saturations and the moisture velocities as

$$\frac{\partial}{\partial t}(\phi S_l \rho_l + \phi S_g \rho_v) = -\frac{\partial}{\partial x}(\rho_l v_l + \rho_v v_v). \tag{2}$$

Conservation of total, non-solid mass in the control volume (liquid plus gas) is obtained as

$$\frac{\partial}{\partial t}(\phi S_l \rho_l + \phi S_g \rho_g) = -\frac{\partial}{\partial x}(\rho_l v_l + \rho_g v_g). \tag{3}$$

Conservation of momentum, wet region

The equations of motion are written for the liquid and gas phases ($i = l, g$). Assumption (8) is applied and the flow process in a porous medium is treated as quasi-steady, that is, the characteristic time for fluid flow in the pore space is small compared to the characteristic times for typical drying processes. The velocities of the gas and liquid phases in a moist porous solid are, respectively,

$$v_g = -\frac{K_{sat} k_{rg}}{\mu_g} \frac{\partial P_g}{\partial x} \tag{4}$$

$$v_l = -\frac{K_{sat} k_{rl}}{\mu_l}\left(\frac{\partial P_l}{\partial x} - \rho_l g\right). \tag{5}$$

The velocities of the individual gas phase components, water vapor and air, are obtained in terms of the mass average velocity of the gas phase given by equation (4) and Fick's law for the diffusion component.

Conservation of energy, wet region

The governing energy equation is for a multi-phase, multi-component porous material

$$(\phi S_l\rho_l c_{Pl}+\phi S_g\rho_v c_{Pv}+\phi S_g\rho_a c_{Pa}+(1-\phi)\rho_s c_{Ps})\frac{\partial T}{\partial t}$$
$$+[\rho_l v_l c_{Pl}+\rho_v v_v c_{Pv}+\rho_a v_a c_{Pa}]\frac{\partial T}{\partial x}$$
$$=\frac{\partial}{\partial x}\left(k_{eff}\frac{\partial T}{\partial x}\right)-\dot{m}h_{vap}. \quad (6)$$

The wet region drying regime is described by equations (1)–(6) in terms of the dependent variables of drying: T, S_l and P_g. Additional thermodynamic and transport property information is required for the complete description of the wet region drying regime.

Conservation of mass, sorption region

During the sorption region drying regime the liquid phase is no longer continuous ($S_l < S^*$) and is bound in the porous solid matrix. The predominant movement of the moisture takes place in the gas phase. As a result of the discontinuity of the remaining liquid phase, the evaporation front recedes from the drying surface into the porous medium. For bound moisture present in the porous solid matrix the conservation of mass equation is written as [19]

$$\frac{\partial}{\partial t}(\phi S_l\rho_l)=-\frac{\partial}{\partial x}(\rho_l v_b)-\dot{m}. \quad (7)$$

This equation differs from equation (1) by the velocity that describes the bound liquid motion in the sorption region. Conservation of total water mass (liquid plus vapor) and total non-solid mass (liquid plus gas) are described in general form by equations (2) and (3), however, the bound moisture velocity and the thermodynamic and transport properties that describe this regime are different than those terms that describe the initial wet region period.

Conservation of momentum, sorption region

In the sorption drying regime, the liquid phase is no longer continuous. Localized moisture is trapped in the porous solid matrix with the flow of liquid to the drying surface nearly depleted. This bound liquid velocity is characterized by the gradient of the volumetric saturation of the bound liquid in the sorption region and the bound moisture properties as

$$v_b=-\phi D_b\frac{\partial S_l}{\partial x} \quad (8)$$

where D_b is the bound water conductivity and describes the ability of the moisture to transport within the matrix during this period of drying.

Conservation of energy, sorption region

The definition of the bound liquid enthalpy is given by [17, 18, 20] as the following

$$h_b=h_l-\Delta h_w \quad (9)$$

or that the enthalpy of the bound liquid is less than that of free liquid by the differential heat of sorption. The energy equation for this drying regime is of the form

$$\left(\phi S_l\rho_l c_{Pl}+\phi S_g\rho_v c_{Pv}+\phi S_g\rho_a c_{Pa}+(1-\phi)\rho_s c_{Ps}\right.$$
$$\left.-\phi\rho_l\int_0^{S_l}\frac{\partial\Delta h_w}{\partial T}\,dS_l\right)\frac{\partial T}{\partial t}-\phi\rho_l\,\Delta h_w\frac{\partial S_l}{\partial t}$$
$$+[\rho_l v_b c_{Pl}+\rho_v v_v c_{Pv}+\rho_a v_a c_{Pa}]\frac{\partial T}{\partial x}-\rho_l v_b\frac{\partial\Delta h_w}{\partial x}$$
$$=\frac{\partial}{\partial x}\left(k_{eff}\frac{\partial T}{\partial x}\right)-\dot{m}(h_{vap}+\Delta h_w) \quad (10)$$

where the differential heat of sorption is defined as

$$\Delta h_w=-\frac{\bar{R}}{M_v}T\ln\frac{P_v}{P_{vs}}. \quad (11)$$

The dependent variables of drying in the sorption 'dryout' region are: T, S_l and P_g. The sorption region transport and thermodynamic properties, like those of the wet region, will be functions of the dependent variables of drying.

TWO REGION DRYING ANALYSIS

The traditional mathematical formulation of the moving boundary problem is to perform mass and energy balances at the receding front in terms of the unknown front velocity. This approach is used in the Stefan problem for melting (or solidification). As shown in [9, 51], the evaporation front that occurs at temperatures below the saturation temperature need not be described by the processes in the Stefan problem. Problems of the Stefan type are described by the continuity and knowledge of the dependent variable (i.e. temperature) and a discontinuity of a thermodynamic property (i.e. enthalpy) at the moving boundary. For drying below the saturation temperature, however, the temperature, moisture concentration, and gas phase pressure as well as all thermodynamic properties are continuous at this location. The moisture content at the receding front is continuous and equal to the maximum sorptive moisture content and is given by $S_l = S^*$.

It is necessarily assumed in this model that the evaporation front recedes uniformly into the porous solid. The front position is determined by S^* and is thus a natural consequence of the solution of the governing conservation equations with the use of the drying region dependent thermodynamic and transport properties such as the relative permeabilities of the gas and liquid phases, vapor pressure, bound liquid conductivity, and bound liquid enthalpy.

The solid backing layer is attached to the moist porous fiber layer at $x = L_l$ (see Fig. 1). The thermal characteristics of the backing material during the drying process are just as important as those of the porous fiber layer due to the temperature sensitivity of the

solid backing material. The transient heat conduction equation with constant properties is written for the solid backing material.

BOUNDARY AND INITIAL CONDITIONS

The characteristics in the partially saturated porous fiber layer and solid-backing material (i.e. T_b, T, S_l, and P_g) are dependent on the conditions imposed on its boundaries. Additionally, since the solution is transient in nature, the initial condition of the material must also be specified. The boundary conditions are obtained from surface mass and energy balances. A surface energy balance is performed at the heat transfer surface, $x = 0$ (i.e. refer to Fig. 1). Mass and energy balances are performed at the attachment location, $x = L_1$. Additionally, temperature continuity is applied at this location. Finally, mass and energy balances are performed at the drying surface, $x = L_2$. Initial conditions are obtained from the specific knowledge of the drying process. The initial conditions are required for the temperature of the materials, the moisture concentration and the gas phase pressure. It is assumed that the initial moisture content is uniformly distributed (based on a limited sample size) throughout the porous layer.

Heat and mass transfer coefficients

The jet impingement drying process dictates the manner and the rate at which the porous solid dries. The boundary conditions governing the heat and mass transfer rates at the drying surface during a continuous industrial during process are modeled using a turbulent multiple jet impingement flow field. In order to obtain the heat and mass transfer correlations for this flow field, one method is to obtain a quantitative relationship for the rate of turbulent energy dissipation in terms of the fluid and geometric characteristics of the multiple impinging jets. A general relationship containing the mechanical energy input to the fluid and additional characteristics of the flow field are necessary to describe a correlation for the turbulent heat and mass transfer rates at the drying surface ($x = L_2$ in Fig. 1).

A heat and mass transfer correlation is obtained by the application of the Kolmogoroff theory of isotropic turbulence [22, 24, 25, 29, 49]. The mechanical energy supplied to the fluid develops into kinetic energy of the integral scale eddies (order of magnitude of the flow field) and is subsequently transferred to the smaller scale eddies where the dissipation occurs. Each step occurs continuously with the small scale eddies in an equilibrium state. Therefore, small scale eddies available for heat and mass transfer depend only on the rate of energy dissipation, ε_t, and the kinematic viscosity, ν, of the fluid, Skelland *et al.* [29]. With this, the Kolmogoroff time scale of the dissipation becomes

$$t_K = \left(\frac{\nu}{\varepsilon_t}\right)^{1/2}. \tag{12}$$

A mass transfer coefficient expression can be obtained with the Higbie penetration theory, Skelland [16]. The penetration theory relates the mass transfer coefficient to the molecular diffusivity (water vapor in air) and the exposure time. The exposure time, t_e, is the amount of time a turbulent eddy (small scale) remains at the liquid (i.e. porous solid surface)–drying air interface (i.e. $x = L_2$) and then returns to the bulk of the drying fluid. It is assumed that the exposure time and the Kolmogoroff time are identical, Skelland [29]. The mass transfer coefficient is written in terms of the rate of energy dissipation and the kinematic viscosity of the fluid with the introduction of the Kolmogoroff time scale for turbulence

$$\bar{h}_m = 2\sqrt{\left(\frac{D}{\pi}\right)\left(\frac{\varepsilon_t}{\nu}\right)^{1/4}}. \tag{13}$$

The mass transfer coefficient is estimated if the rate of the turbulent energy dissipation can be obtained from the flow field developed by the multiple impinging jet geometry. Equation (13) is written in terms of the Schmidt number as

$$\bar{h}_m = \frac{2}{\sqrt{\pi}} DSc^{1/2} \frac{(\varepsilon_t \nu)^{1/4}}{\nu}. \tag{14}$$

The Reynolds analogy is applied for a turbulent flow field to obtain the heat transfer coefficient in the following general form

$$\bar{h}_T = \frac{2}{\sqrt{\pi}} k_{g\infty} Pr^{1/2} \frac{(\varepsilon_t \nu)^{1/4}}{\nu} \tag{15}$$

where the fluid and thermal properties such as thermal conductivity, viscosity, and specific heat are evaluated as humid air properties, that is, a binary mixture of ideal gases. The heat transfer coefficient at the solid backing surface is taken as a percentage of the drying surface coefficient.

The establishment of the rate of turbulent energy dissipation, ε_t, requires the knowledge of the mechanical energy input to the fluid. The turbulent energy dissipation is defined in general as

$$\varepsilon_t \equiv \frac{\text{mechanical energy input}}{\text{mass of fluid}}. \tag{16}$$

The total mechanical energy input to the flow field (the drying air) includes the blower power, $\dot{W}_b$, and the acceleration of the fluid through the nozzle-jet system. The turbulent energy dissipation to the surrounding fluid interaction in the dryer is written in terms of the blower power and the jet velocity per unit mass of fluid as

$$\varepsilon_t = (1 - C_1) \frac{\dot{W}_b + \frac{1}{2} N \dot{m}_{jet} V_{jet}^2}{m_v + m_a} \tag{17}$$

where the constant is constrained by $0 < C_1 < 1$. The decay of the turbulent energy dissipation within the jet itself is an important feature that relates the tur-

bulence dissipation rate to the nozzle-to-product separation distance, H (refer to Fig. 1). It is assumed, for small separation distances, that the amount of mass entrained into the jet from the surrounding stationary air is negligible, Baughn *et al.* [52] and Goldstein *et al.* [53]. Therefore, equation (17) must reflect the decay of the rate of turbulent energy dissipation within the jet itself. This final effect is estimated by the theory of grid (or source) generated turbulence.

For high Reynolds number ranges, grid generated turbulence models produce energy decay relationships downstream of the initial source of turbulence. During the initial period of turbulent decay, the root mean square of the velocity fluctuation is a function of the distance from the source and the differentiation of the velocity with respect to this distance provides for the rate of turbulent energy dissipation. The rate of dissipation of turbulent energy decays as the inverse square of the distance from the source of the turbulence.

An estimate for the rate of decay of turbulence energy dissipation within the impinging jets and to the surrounding fluid near the drying surface is

$$\varepsilon_t = (1-C_l)\frac{\dot{W}_b + \frac{1}{2}N\dot{m}_{jet}V_{jet}^2}{m_v + m_a}\left(\frac{H}{S_d} - \left(\frac{H}{S_d}\right)_0\right)^{-2} \tag{18}$$

where S_d is the nozzle-to-nozzle spacing and H is the nozzle-to-product separation and $(H/S_d)_0$ is the virtual origin obtained in terms of the jet Reynolds number

$$Re_d = \frac{NV_{jet}d}{v}$$

where d is the nozzle (or hole) diameter. With this approximate expression for the turbulent energy dissipation rate, heat and mass transfer rates at the drying surface may be estimated.

The conservation equations and the boundary conditions must be supplemented with thermodynamic and transport properties describing the appropriate drying regimes and the transport of moisture (liquid and vapor) and energy during the drying process.

THERMODYNAMIC AND TRANSPORT PROPERTIES

The governing equations of mass, momentum and energy developed for the moist porous fiber medium contain numerous thermodynamic properties of the fluid constituents in the porous solid. Transport properties based on the geometry of the porous solid inherently govern the flow of the constituent fluids and ultimately the manner in which the solid is dried. Thermodynamic and transport properties must be established for the wet region drying period and the sorption region period. These drying regional property (thermodynamic and transport) differences establish the position of the evaporation front during the drying process.

The equations of state

The densities of the individual components, water vapor, air and gas phase, are obtained by the ideal gas law assumed valid for the water vapor in air mixture at the low pressures of the tests.

Vapor pressure relationships

The vapor pressure relationship during the wet region drying conditions (i.e. free liquid water in the porous solid) can be obtained with the Clausius–Clapeyron equation, Kaviany [15]. During the sorption region drying period the desorption isotherm obtained from [1] is

$$\frac{P_v}{P_{vs}} = 1 - \exp\left(-(154.4 - 0.359T) \times \left(\frac{\rho_l S_l \phi}{\rho_s(1-S_l\phi)}\right)^{(4.51-0.008T)}\right) \tag{19}$$

where P_{vs} is the saturation vapor pressure given by the Clapeyron equation. This vapor pressure lowering curve obtained from the literature was found to provide adequate results when applied to the drying model used in the laboratory batch drying process.

Capillary pressure relationships

The capillary pressure curve $P_c = P_c(S_l, T)$ is obtained from Preston and Nimkar [54] for a fiber material where the temperature dependence is small compared to the moisture concentration, Francis [19]. This relationship was found to adequately represent the early stages of drying (i.e. wet region period) during the small scale dryer model validations, Francis [19].

Relative permeabilities

The relative permeabilities of the liquid and gas phases are determined by Dullien [55] as

$$k_{rl} = (S_{eff})^{(2+3\lambda)/\lambda} \tag{20}$$

$$k_{rg} = (1-S_{eff})^2(1-S_{eff})^{(2+\lambda)/\lambda} \tag{21}$$

where

$$S_{eff} = \left(\frac{P_{cb}}{P_c}\right)^{\lambda} (P_c \geqslant P_{cb}). \tag{22}$$

The bubbling pressure and the pore size distribution index are determined from the capillary pressure curve vs the moisture saturation of the material plotted on a log–log scale. The bubbling pressure and pore size distribution index are $P_{cb} = 1258.0$ N m^{-2} and $\lambda = 0.6$, respectively. The absolute permeability, K_{sat}, is the transport parameter for single phase flow in porous materials and is obtained from Van Den

Brekel and DeJong [56] as an average $K_{sat} = 4.4 \times 10^{-11}$ m^2.

Molecular diffusivity

The effective diffusivity for water vapor diffusion through a fabric as obtained by Whelan *et al.* [57] is

$$D_{eff} = \frac{D}{\frac{4.3}{\phi} - 3.4} \tag{23}$$

where D is the molecular diffusion coefficient for water vapor in air and ϕ is the porosity of the porous textile sample.

Bound moisture conductivity

Chen and Pei [1] recommend the following Arrhenius-type function of temperature of the porous solid as

$$D_b = D_{b_0}(S_l) \exp\left(-\frac{E_d}{\bar{R}T}\right) \tag{24}$$

where E_d is the activation energy of movement of bound liquid moisture. The bound moisture coefficient is of the following form

$$D_{b_0}(S_l) = \text{const}_1\left(\frac{S_l - S_{eq}}{S^* - S_{eq}}\right)^{\text{const}_2} \tag{25}$$

where the constants are varied for different solid material types and pore geometries.

Thermal conductivity

The thermal conductivity is modified for the transfer of energy by conduction through a multiphase porous material. The effective porous thermal conductivity can be idealized to be in a parallel format as recommended by Naka and Kamata [58] for moist textile materials

$$k_{eff} = \phi(1 - S_l)k_g + \phi S_l k_l + (1 - \phi)k_s. \tag{26}$$

NUMERICAL ANALYSIS

The dependent variables of drying are nondimensionalized and the governing equations written in a dimensionless format, with the details given in Francis [19]. Dimensionless forms of mass and energy transport for both drying regimes and the associated boundary conditions are discretized using a finite difference format written in computational form via the Patankar method, [59]. The equations are linearized by evaluating the coefficients at the previous time step. This technique, however, places restrictions on the time step and grid size necessary to obtain convergence of the system of equations. The dimensionless numerical criteria given by $r = \Delta t^*/\Delta x^{*2} = 1/2$ must be satisfied during the computations in order to obtain convergence of the system of equations. As a result of the jet impingement boundary condition (i.e. large heat and mass transfer coefficients at the drying surface) and increased drying temperatures, enhanced convective flows in the porous material require a finer spatial grid than that required by the small scale dryer model in which conduction is the dominant mode of heat transfer. Convection increases in the partially saturated porous solid are a direct result of increased temperature and pressure gradients in the solid. These requirements necessitate small time steps.

Solution of the governing equations

The governing system of simultaneous algebraic equations developed in terms of dimensionless parameters T_b^*, S_l, θ and P_g^* are in the special form of a quad-tridiagonal system of equations, Von Rosenberg [60]. A very general form of the linearized system of equations is

$$\sum_l a_l^k \Psi_{i-1}^l + b_l^k \Psi_i^l + c_l^k \Psi_{i+1}^l = d^k \tag{27}$$

where Ψ is the dimensionless dependent variable and a, b, c and d are the kinetic and capacity coefficients corresponding to the appropriate conservation equation. The indices are described as follows. The conservation equation index, $k = 1, 2, 3, 4$, where 1 = total water mass, 2 = total (non-solid) mass, 3 = energy (porous medium), 4 = energy solid backing. The variable index $l = 1, 2, 3, 4$, where 1 = volumetric saturation, 2 = temperature (porous medium), 3 = gas phase pressure, 4 = temperature (solid backing). The spatial index is given by i. The system of equations are simplified depending on the domain of interest. For example, in the solid backing layer, $0 \leqslant x < L_1$, the dependent variable of interest is the temperature distribution in the solid. Therefore, at any node (i) in the backing solid, the porous material variables are: $S_l = \theta = P_g^* = 0$. In the porous medium, the backing layer temperature, $T_b^* = 0$, and the leading coefficients pertaining to this variable are not relevant in the domain $L_1 < x \leqslant L_2$. $x = L_1$ serves as the coupling location for the systems of equations used to model the composite material subjected to an industrial drying process.

EXPERIMENTAL PROCEDURES

The continuous feed industrial dryer is characterized by the continuous motion of the moist textile product through the oven and by the turbulent jet impingement boundary condition at the drying surface. The thermal characteristics of the material are greatly affected by the flow field and its impact on the heat and mass transfer coefficients. A schematic of the general features of this drying analysis is shown in Fig. 1. Instrumentation of the moist product is shown with pertinent flow field geometric and fluid characteristics such as jet velocity, belt speed, and nozzle spacing. The partially saturated textile com-

posite is an 18 × 18 inch square approximately 1/4 to 1/3 inch thick.

During the continuous industrial drying process, the drying medium impinges directly onto the moist modular carpet tile. Due to the presence of the solid backing layer, it is assumed that the flow field does not penetrate the solid. This assumption is found to hold also in a simple batch drying process performed in the laboratory experiment. The jet velocity from a single nozzle in banks of nozzle arrays is denoted by V_{jet}. The distance between the nozzle array system and the porous material being dried is denoted by H in Fig. 1. The top surface ($x = L_2$) is a heat and mass transfer boundary while the lower surface ($x = 0$) is a heat transfer boundary only. The oven air temperature, $T_{\infty,n}$, is a function of position in the dryer and can be varied for different drying processes. It is assumed in this work that the industrial dryer operates as a steady state device, that is, the amount of mass (water vapor and dry air) in the dryer zone remains essentially constant.

Temperature data within the porous solid are obtained during the continuous industrial drying process at specific points in the moist porous fiber and solid backing layers. In this case, wireless needle probes are preprogrammed and positioned into the composite material to take and store temperature data during the drying process. Two needle probes are used to measure temperature at discrete points; one in the solid backing layer and one in the moist porous fiber layer (refer to Fig. 1). Moisture concentration data cannot be continuously measured for this dryer type. In this case, the textile product is removed from the dryer on a zone-to-zone basis and individually weighed. The average moisture content profile is obtained over the length of the dryer based on zone position. In this analysis, experimental temperature profiles and global moisture concentration data are obtained for different initial moisture contents, oven air temperatures and belt speeds.

The process parameters for the continuous industrial dryer are: the initial moisture content of the porous solid, the constant belt velocity V_{belt}, and the zone temperatures $T_{\infty,n}$. The belt velocity characterizes the continuous feed nature of the industrial dryer, that is, the motion (continuous) of the product through the dryer.

RESULTS AND DISCUSSION

The experimental temperature data obtained in the partially saturated porous fiber and solid backing layers are illustrated in Figs. 2(a) and (b) for variable oven air temperatures. The model results are compared directly to experimental temperature data in Figs. 2(a) and (b) and moisture content data in Fig. 3. In order to study the effect of the surrounding fluid turbulent energy dissipation on the heat and mass transfer coefficients obtained for this dryer type, Table 1 is given with a variable C_1 and model results are shown in Figs. 2 and 3. The mass and heat transfer coefficients for this dryer type are obtained with the use of equations (14) and (15) with equation (18) evaluated as the turbulence energy dissipation term. The surrounding fluid dissipation coefficient varies as $(1-C_1)^{1/4}$. Figures 2(a) and (b) are obtained for a surrounding fluid dissipation term of 0.0266 and the dryer parameters as specified in the figure captions. Table 1 indicates the flow field parameters considered in this paper.

In this case, it is noted that as C_1 (Fig. 3) < C_1 (not shown) < C_1 [Figs. 2(a) and (b)] → 1.0, the majority of the turbulent energy dissipation is to the surrounding fluid as secondary stagnation regions and fluid interactions are developed by the multiple impinging flows. The turbulence dissipation occurring in the surrounding fluid is assumed lost or greatly reduced for

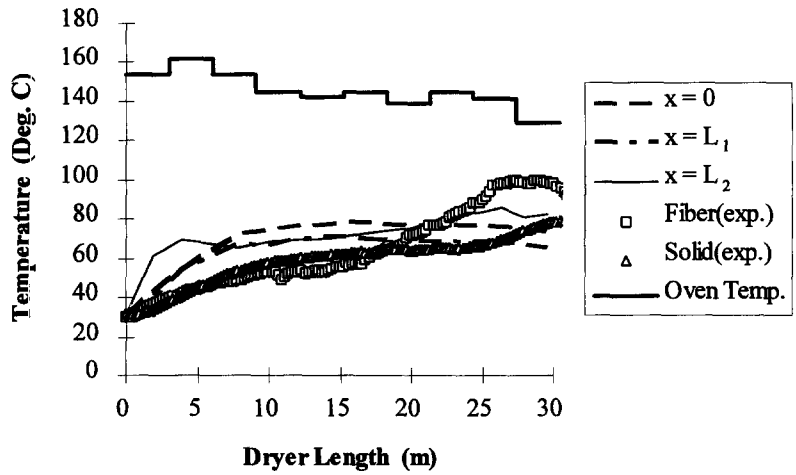

Fig. 2(a). Temperature profile for an industrial dryer, $V_{belt} = 0.079$ m s^{-1}, $X_{l_i} = 0.62$, $T_i = 31.1$°C, $x = 0$ solid-backing adjacent to oven air (model), $x = L_1$ attachment point between fiber and solid (model), $x = L_2$ top fiber drying surface (model).

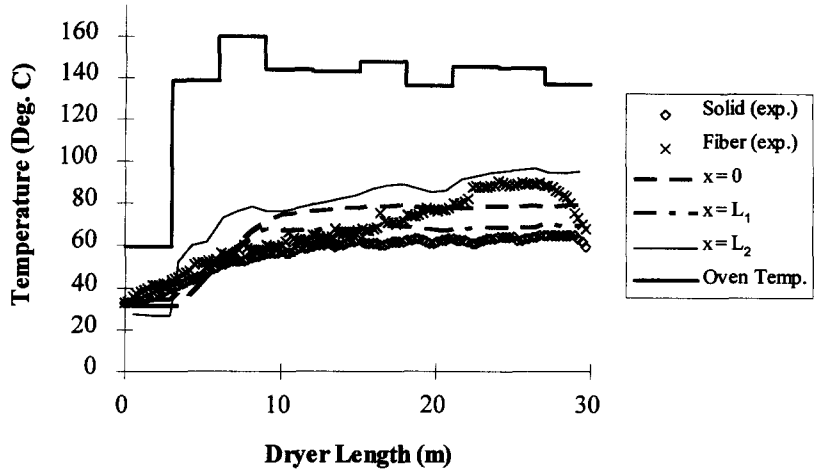

Fig. 2(b). Temperature profile for an industrial dryer, $V_{belt} = 0.082$ m s^{-1}, $X_{l_1} = 0.47$, $T_l = 31.1$°C, $x = 0$ solid-backing adjacent to oven air (model), $x = L_1$ attachment point between fiber and backing (model), $x = L_2$ top fiber drying surface (model).

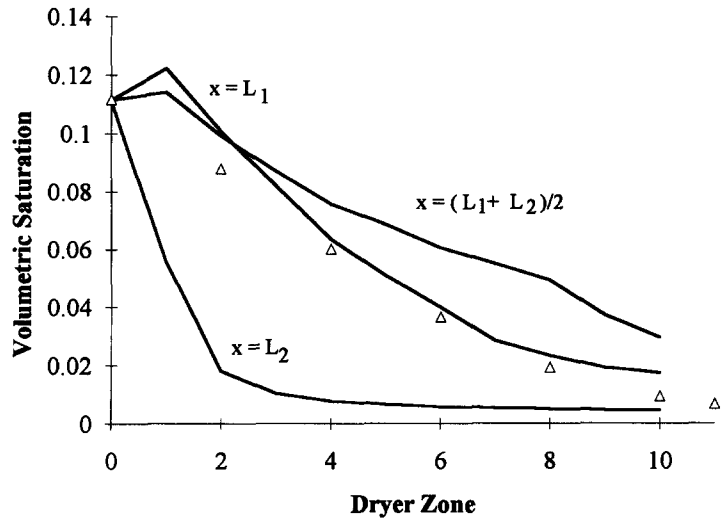

Fig. 3. Moisture content profile for an industrial dryer, $V_{belt} = 0.076$ m s^{-1}, $X_{l_1} = 0.70$, $T_l = 29.4$°C, $x = L_1$ is the attachment point between fiber and backing (model), $x = L_2$ is the top fiber drying surface (model). Δ = global experimental moisture content.

future mass transfer purposes. The heat flux at the surface of the material is important in that it establishes the manner in which the porous solid is dried. For the indicated heat and mass flux conditions, model results are plotted for the solid-backing surface adjacent to the flow field ($x = 0$), the attachment point between moist porous and solid backing layers ($x = L_1$), and finally the fiber surface adjacent to the impingement (drying) boundary ($x = L_2$).

Table 1. Jet impingement heat and mass transfer coefficients

Figure	$(1-C_l)^{1/4}$	$\bar{h}_T$ [W m^{-2} K^{-1}]	$\bar{h}_m$ [m s^{-1}]
2a	0.0266	21	0.023
2b	0.0266	21	0.023
Not shown	0.0473	37	0.042
3	0.0841	66	0.074

The initial temperature rise in the porous fiber [Fig. 2(a)] results from transport phenomena occurring during the wet region period of drying. First, the fluid convection processes within the porous solid as a result of the high heat flux boundary condition (high heat transfer coefficient and oven air temperature) approach the order of the energy diffusion process. Therefore, in the case of impingement drying, the increased velocities of the free liquid phase (wet region drying regime) and the gas phase significantly contributes to the total energy (convection and diffusion) transfer process.

The increased liquid and gas phase transport during the wet region drying period (i.e., the initial stages of

drying) are not sufficiently described by Darcy's law due to the increased gas phase pressure gradients driving both phases. The pore space fluid velocities are increased as a result of these conditions but are underpredicted by the current momentum relationship. Therefore, the temperature changes of the porous material as described by the model are greater than the experimental data as the transport of the liquid heat capacity is not maintained.

The initial increase in temperature predicted by the model may also be a result of the turbulent flow field heat and mass transfer coefficients predicted by the Kolmogoroff theory. In order to provide a basis for the establishment of the jet impingement transfer coefficients, the correlations obtained by the Kolmogoroff theory of isotropic turbulence are compared to empirical results obtained by Martin [21] and Polat [61] on the order of $h_T = 130$ W m^{-2} K^{-1} and $h_m = 0.15$ m s^{-1}.

Table 1 maps the dissipation coefficient C_1 with its corresponding transport coefficients. The velocities of the liquid and gas phases are reduced in the model as the temperature and more importantly the pressure gradients are reduced with decreasing heat transfer at the drying surface. The energy diffusion mechanism in the solid becomes increasingly more important as the external heat flux is reduced and the fluid velocities approach the Darcy regime. The Darcy regime, however, lacks the ability to sufficiently convection cool the material from the wet region.

The moisture content experiment is characterized by oven air temperatures similar to those of Fig. 2. The exact parameters for initial moisture content, temperature, and belt speed are give in Fig. 3. The fluid dissipation coefficient for the drying experiment is obtained in Table 1 where the heat and mass transfer coefficients are obtained from the Kolmogoroff theory. These results indicate extreme drying rates at the surface with moisture redistribution near the solid backing (interior solid) indicating the increased importance of the convective fluid transport early in the drying process.

From Figs. 2 and 3, it is noted that the empirical results of [21, 61] will over predict the mass and heat transfer rates for this drying process according to the results of Table 1. The dissipation of turbulent energy to the surrounding fluid will reduce the drying rates at the surface of the material. This result is captured by the Kolmogoroff theory of isotropic turbulence.

CONCLUSIONS

With the application of Assumption (9), the multiple jet impingement drying analysis (i.e. a high heat flux boundary condition) may be achieved with this model computing Kolmogoroff heat and mass transfer coefficients at the drying surface. Uncertainties exist, however, in this model as for the proper selection of the fluid dissipation coefficient and thus the heat and mass transfer coefficients used to describe the jet impingement flow field. Uncertainties also exist in the application of the thermodynamic and transport properties taken from the literature for this material. However, with the results of Figs. 2 and 3, the lower transport coefficients at the drying surface better represent the experimental data obtained from this particular industrial drying process.

The continuous industrial drying process investigated in this paper is characterized by a turbulent flow field at the drying surface. In this analysis, the oven temperatures and the heat transfer coefficients are much greater than in a typical batch dryer process [19]. The increased heat flux at the surface was seen to significantly affect the internal transport phenomena in the porous material. The model developed for the impingement drying process was compared to experimental analyses for global moisture content and temperature distributions taken directly from an industrial drying process. In order to provide a new estimate for the heat and mass transfer coefficients for a turbulent drying process, the Kolmogoroff theory of isotropic turbulence was employed to provide transport coefficients for the specified nozzle arrays. The new transport coefficients are then compared to known correlations for multiple impinging jets. It is noted that the existing correlations [21] may overestimate the drying rates for this specific dryer.

The increased temperature and gas phase pressure gradients in the porous solid during the wet region drying period (initial stages of drying) necessarily increase the thermal convection terms in the conservation of energy equation during this drying regime. As a result of the analysis presented for the continuous drying processes, it is noted that:

(1) The internal fluid (liquid and gas phases) transport in the high heat flux dryer (i.e. the continuous industrial drying process) must include inertial effects for higher flow velocities. As result, it may be necessary to solve the volume averaged forms of the Navier–Stokes equations in a porous solid in order to accurately account for the higher velocity flow regimes during the wet region drying period.

(2) The heat and mass transfer coefficients for the multiple jet impingement dryer have been obtained from the Kolmogoroff theory of isotropic turbulence. The drying results obtained from the model are seen to approach the experimental data for a variable surrounding fluid dissipation coefficient. In order to test this modeling approach, experimentally determined heat and mass transfer coefficients under the jet impingement drying conditions can be used to establish the drying rates for this dryer type. This work is yet unreported in the literature and is presumed yet undone.

This working model will provide information for the continuous industrial drying process and the drying kinetics associated with this dryer type. This work provides new expressions for the heat and mass transfer coefficients for a multiple jet impingement bound-

ary condition. The transport coefficient correlations are directly applied in a working drying theory for a continuous industrial drying process. This theory is subsequently verified by experimental analyses.

The jet impingement model can be used as a baseline tool to establish the drying characteristics for the high temperature dryer. Temperature, gas phase pressure, and moisture content information can be obtained to provide a basis for dryer design and also aid in process control of existing industrial dryers.

Acknowledgements—The authors wish to acknowledge Dr Joseph J. Smrekar of Milliken and Co. for his invaluable advice on this project and Milliken and Co. for generous support of this work.

REFERENCES

1. P. Chen and D. C. T. Pei, A mathematical model of drying processes, *Int. J. Heat Mass Transfer* **32**(2), 297–310 (1989).
2. P. Chen and P. S. Schmidt, An integral model for drying of hygroscopic and non-hygroscopic materials with dielectric heating, *Drying Technol.* **8**(5), 907–930 (1990).
3. R. M. Perkin, The drying of porous materials with electromagnetic energy generated at radio and microwave frequencies, *Prog. Filtration Separation* **3,** 205–266 (1983).
4. M. A. Roques and A. R. H. Cornish, Phenomenological coefficients for heat and mass transfer equations in wet porous media, *Drying* 1980 **2,** 36–42 (1980).
5. R. Toei, Drying mechanism of capillary porous bodies, *Adv. Drying* **2,** 269–297 (1983).
6. J. Van Brakel, Mass transfer in convective drying, *Adv. Drying* **1,** 217–267 (1980).
7. S. Bories, Recent advances in modelisation of coupled heat and mass transfer in capillary-porous bodies, *Drying*, 46–62 (1989).
8. T. Z. Harmathy, Simultaneous moisture and heat transfer in porous systems with particular reference to drying, *Ind. Engng Chem. Fundam.* **8,** 92–103 (1969).
9. J. G. Hartley, Coupled heat and moisture transfer in soils: a review, *Adv. Drying* **4,** 199–248 (1987).
10. C. Moyne and P. Perre, Processes related to drying—I. Theoretical model, *Drying Technol.* **9**(5), 1135–1152 (1991).
11. S. B. Nasrallah and P. Perre, Detailed study of a model of heat and mass transfer during convective drying of porous media, *Int. J. Heat Mass Transfer* **31**(5), 957–967 (1988).
12. M. Quintard and J. R. Puiggali, Numerical modelling of transport processes during the drying of a granular porous medium, *Heat Technol.* **4**(2), 37–57 (1986).
13. S. Whitaker, Simultaneous heat, mass and momentum transfer in porous media: a theory of drying, *Adv. Heat Transfer* **13,** 119–203 (1977).
14. R. B. Bird, W. E. Stewart and E. N. Lightfoot, *Transport Phenomena*, Chap. 15. John Wiley, New York (1960).
15. M. Kaviany, *Principles of Heat Transfer in Porous Media*. Springer, Berlin (1991).
16. A. H. P. Skelland, *Diffusional Mass Transfer*, Chap. 2. R. E. Krieger, Malabar, FL (1985).
17. P. Perre, J. P. Fohr and G. Arnaud, A model of drying applied to softwoods: the effect of gaseous pressure below the boiling point, *Drying*, 91–98 (1989).
18. M. Fortes and M. R. Okos, A non-equilibrium thermodynamics approach to transport phenomena in capillary porous media, *Trans. ASAE* **24,** 756–760 (1981).
19. N. D. Francis, Heat and mass transfer in a semi-porous textile composite, Ph.D. Thesis, Georgia Institute of Technology, Atlanta, GA (1994).
20. R. B. Keey, *Introduction to Industrial Drying Operations*, Chap. 2. Pergamon Press, Oxford (1978).
21. H. Martin, Heat and mass transfer between impinging gas jets and solid surfaces, *Adv. Heat Transfer* **13,** 1–60 (1977).
22. P. H. Claderbank and M. B. Moo-Young, The continuous phase heat and mass-transfer properties of dispersions, *Chem. Engng Sci.* **16,** 39–54 (1961).
23. P. Harriott, Mass transfer to particles—I. Suspended in agitated tanks; II. Suspended in a pipeline, *A.I.Ch.E. Jl* **8**(8), 93–102 (1962).
24. Y. Kawase and M. Moo-Young, Solid-turbulent fluid heat and mass transfer: a unified model based on the energy dissipation rate concept, *Chem. Engng J.* **36,** 31–40 (1987).
25. K. Kikuchi, T. Sugawara and H. Ohashi, Correlation of liquid-side mass transfer coefficient based on the new concept of specific power group, *Chem. Engng Sci.* **43**(9), 2533–2540 (1988).
26. C. J. King, Turbulent liquid phase mass transfer at a free gas–liquid interface, *Ind. Engng Chem. Fundam.* **5**(1), 1–8 (1966).
27. S. Middleman, Mass transfer from particles in agitated systems: application of the Kolmogoroff theory, *A.I.Ch.E. Jl* **11**(4), 750–752, 760–761 (1965).
28. B. D. Prasher and G. B. Wills, Mass transfer in an agitated vessel, *Ind. Engng Chem. Process Des. Dev.* **12**(3), 351–354 (1973).
29. A. H. P. Skelland and J. M. Lee, Drop size and continuous-phase mass transfer in agitated vessels, *A.I.Ch.E. Jl* **27**(1), 99–111 (1981).
30. G. R. Hadley, Numerical modeling of the drying of porous materials, *Proceedings of the Fourth International Drying Symposium*, Vol. 1, pp. 151–158, 9–12 July (1984).
31. C. L. D. Huang, H. H. Siang and C. H. Best, Heat and moisture transfer in concrete slabs, *Int. J. Heat Mass Transfer* **22,** 257–266 (1979).
32. R. M. Perkin, Simplified modelling for the drying of a non-hygroscopic capillary porous body using a combination of dielectric and convective heating, *Drying Technol.* **8**(5), 931–951 (1990).
33. J. A. Rogers and M. Kaviany, Funicular and evaporation-front regimes in convective drying of granular beds, *Int. J. Heat Mass Transfer* **35**(35), 469–480 (1992).
34. I. W. Turner and P. G. Jolly, Combined microwave and convective drying of a porous material, *Drying Technol.* **9**(5), 1209–1269 (1991).
35. K. M. Waananen, J. B. Litchfield and M. R. Okos, Classification of drying models for porous solids, *Drying Technol.* **11**(1), 1–40 (1993).
36. S. Whitaker, Heat and mass transfer in granular porous media, *Adv. Drying* **1,** 23–61 (1980).
37. S. Whitaker, Moisture transport mechanisms during the drying of granular porous media, *Drying*, 21–32 (1985).
38. S. Whitaker and W. T. H. Chou, Drying granular porous media—Theory and experiment, *Drying Technol.* **1**(1), 3–33 (1983).
39. N. D. Francis and W. J. Wepfer, Experimental and numerical analysis of the drying characteristics of modular carpet tiles, *Textile Res. J.* **63**(1), 1–13 (1993).
40. M. Ilic and I. W. Turner, Convective drying of a consolidated slab of wet porous material, *Int. J. Heat Mass Transfer* **32**(12), 2351–2362 (1989).
41. M. Ilic and I. W. Turner, A continuum model of drying processes involving a jump through hysteresis, *Drying Technol.* **9**(1), 79–111 (1991).
42. A. V. Luikov, *Heat and Mass Transfer in Capillary-Porous Bodies*. Pergamon Press, Oxford (1966).
43. A. V. Luikov, Systems of differential equations of heat

and mass transfer in capillary-porous bodies, *Int. J. Heat Mass Transfer* **18,** 1–14 (1975).
44. I. W. Turner and M. Ilic, Convective drying of a consolidated slab of wet porous material including the sorption region, *Int. Comm. Heat Mass Transfer* **17**(1), 39–48 (1990).
45. Z. Prezesmycki and C. Strumillo, The mathematical modelling of drying process based on moisture transfer mechanism, *Proceedings of the Fourth International Drying Symposium*, Vol. 1, pp. 151–158, 9–12 July (1984).
46. S. Polat, B. Huang, A. S. Majumdar and W. J. M. Douglas, Numerical flow and heat transfer under impinging jets: a review, *Ann. Rev. Numer. Fluid Mech. Heat Transfer* **2,** pp. 157–197 (1989).
47. S. Polat, A. S. Mujumdar, A. R. P. van Heiningen and W. J. M. Douglas, Effect of near-wall modelling on prediction of impingement heat transfer, *Drying Technol.* **8**(4), 705–730 (1990).
48. S. Polat, A. S. Mujumdar, A. R. P. van Heiningen and W. J. M. Douglas, Numerical model for turbulent jets impinging on a surface with throughflow, *J. Thermophys. Heat Transfer* **5**(2), 172–180 (1991).
49. Y. Kawase, The energy dissipation rate concept for turbulent heat and mass transfer in drag-reducing fluid, *Int. Commun. Heat Mass Transfer* **17,** 155–166 (1990).
50. A. L. Kistler and T. Vrebalovich, Grid turbulence at large Reynolds numbers, *J. Fluid Mech.* **26,** 37–47 (1966).
51. R. J. Couvillion, Heat and mass transfer in a semi-infinite moist soil with a drying front present, Ph.D. Thesis, Georgia Institute of Technology, Atlanta, GA (1981).
52. J. W. Baughn, A. E. Hechanova and X. Yan, An experimental study of entrainment effects on the heat transfer from a flat surface to a heated circular impinging jet, *J. Heat Transfer* **113,** 1023–1025 (1991).
53. R. J. Goldstein and W. S. Seol, Heat transfer to a row of impinging circular air jets including the effect of entrainment, *Int. J. Heat Mass Transfer* **34**(8), 2133–2147 (1991).
54. J. M. Preston and M. V. Nimkar, Capillary phenomena in assemblies of fibres, *J. Textile Inst.* **43,** T402–T422 (1952).
55. F. A. L. Dullien, *Porous Media Fluid Transport and Pore Structure*, Academic Press, London (1979).
56. L. D. M. Van Den Brekel and E. J. De Jong, Hydrodynamics in packed beds, *Textile Res. J.* **59,** 433–440 (1989).
57. M. E. Whelan, L. E. MacHattie, A. C. Goodings and L. H. Turl, The diffusion of water vapor through laminae with particular reference to textile fabrics, *Textile Res. J.* **25**(3), 197–2323 (1955).
58. S. Naka and Y. Kamata, Thermal conductivity of wet fabrics, *J. Textile Mach. Soc. Jpn* **23**(4), 114–119 (1977).
59. S. V. Patankar, *Numerical Heat Transfer and Fluid Flow*. McGraw–Hill, Maidenhead, U.K. (1980).
60. D. U. Von Rosenberg, *Methods for the Numerical Solution of Partial Differential Equations*. American Elsevier Publ. Co., New York (1969).
61. S. Polat, Heat and mass transfer in impingement drying, *Drying Technol.* **11**(6), 1147–1176 (1993).